

8
3
4

#1

V393
.R46



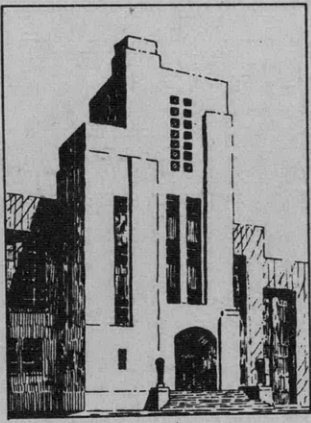
NAVY DEPARTMENT

THE DAVID W. TAYLOR MODEL BASIN

WASHINGTON 7, D.C.

STEADY TWO-DIMENSIONAL CAVITY FLOWS
ABOUT SLENDER BODIES

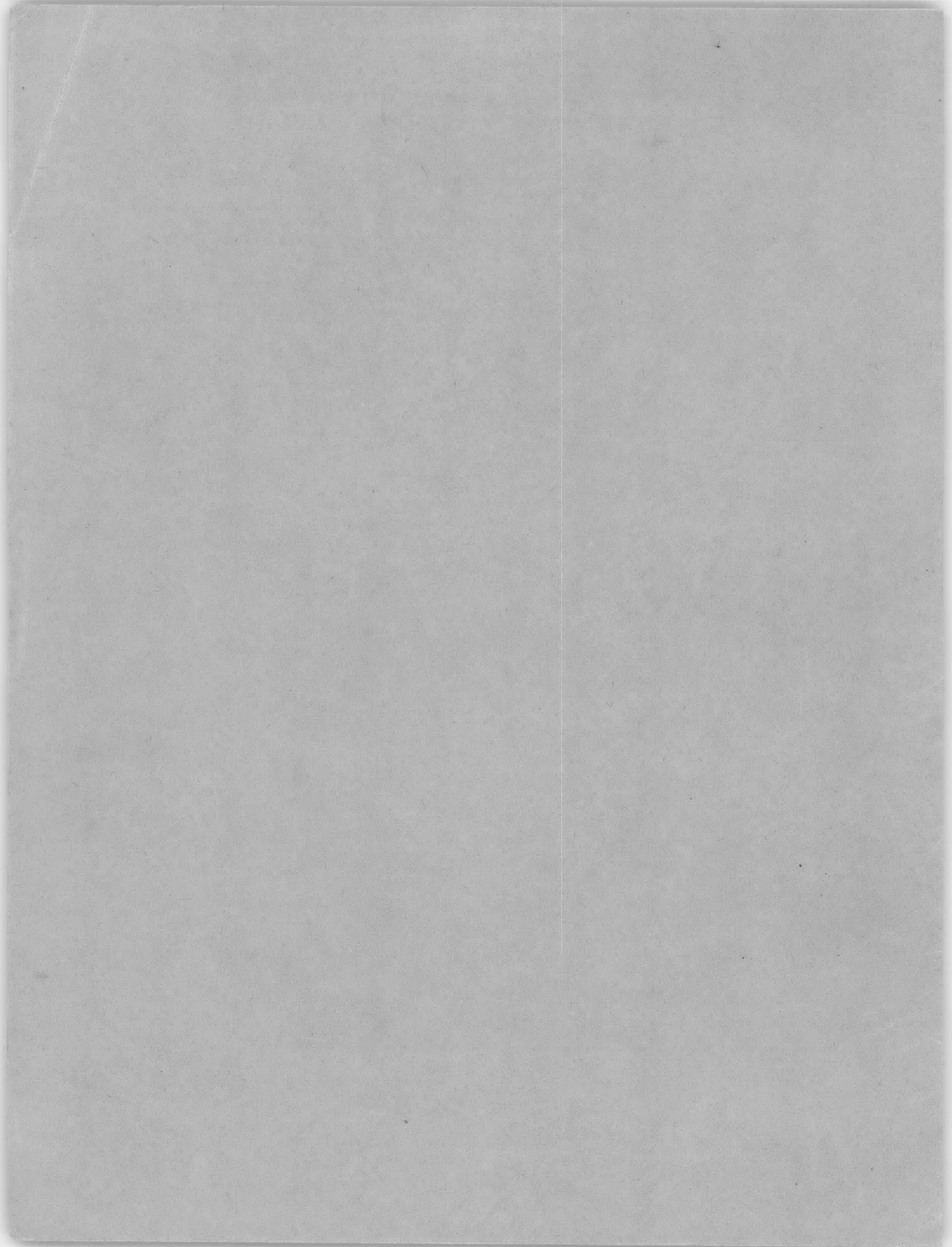
by
M. P. Tulin



May 1953

Report 834

NS 715-102



STEADY TWO-DIMENSIONAL CAVITY FLOWS ABOUT SLENDER BODIES

by

M.P. Tulin

May 1953

Report 834

NS715-102

NOTATION

a	A constant, undefined in terms of physical parameters
C_D	Drag coefficient
c	Body chord length
D	Drag or resistance
$D_{\sigma=0}$	Drag for zero cavitation number
k	Strength of vorticity distribution
L	Length of cavity measured from body leading edge
l	Length of cavity measured from body trailing edge
m	Strength of source distribution
p	Local static pressure
p_c	Cavity pressure
p_0	Pressure on the body
p_∞	Static pressure of stream at infinity
R	Denotes "the real part of"
s	Mathematical parameter, undefined in terms of physical parameters
T	Maximum thickness of wedge profile
t	Dummy variable
U_c	The x -component of the velocity on the cavity
U_0	The x -component of the velocity on the body
U_∞	The uniform velocity at infinity, parallel to the x -axis
u	The x -component of the disturbance velocity, \vec{v}
u_{c-0}	The x -component of the disturbance velocity on the body which is induced by the cavity source distribution.
u_{0-0}	The x -component of the disturbance velocity on the body which is induced by the body source distribution.
\vec{V}	The velocity of the fluid, at any point in the flow field.

\vec{v}	The local disturbance velocity, $\vec{V} - U_\infty$
v	The y -component of the disturbance velocity
v_c	The y -component of the disturbance velocity on the cavity
v_0	The y -component of the disturbance velocity on the body
x	A space coordinate, in the direction of the plane of body symmetry and parallel to U_∞
x'	A dummy variable
\bar{x}	The distance from the body trailing edge to position of maximum cavity thickness
y	A space coordinate, orthogonal to the x -direction and to the plane of body symmetry
y_c	Semi-thickness of the cavity
y_0	Semi-thickness of the body
γ	Wedge profile half angle
ρ	Fluid density
σ	Cavitation number
τ	Dummy variable
ϕ	Velocity potential
χ	Dummy variable

TABLE OF CONTENTS

	Page
ABSTRACT	1
INTRODUCTION	1
THE LINEARIZED THEORY	2
THE THIN AIRFOIL THEORY AND THE JUNCTURE CONDITION	6
THE GENERAL SOLUTION FOR THE SOURCE DISTRIBUTION AND CAVITY SHAPE	7
THE CALCULATION OF THE CAVITATION DRAG	10
THE INFINITE CAVITY CASE ($\sigma = 0$)	11
THE SLENDER WEDGE - COMPARISON WITH EXACT THEORY	12
SUMMARY AND CONCLUSIONS	13
APPENDIX 1 -	18
A. Useful Integrals	18
B. A Proof of a Result used in the Derivation of Equation [19]	19
C. Listing of Useful Theoretical Results	19
REFERENCES	20

ABSTRACT

A linearized theory is developed for steady, two-dimensional cavity flows about slender symmetric bodies. The theory is applied to the cases of zero and nonzero (positive) cavitation numbers. It is shown that, for the case of finite cavities, the linearized theory avoids the necessity for choosing an artificial cavitation model as must be done in any exact theory attempts. The problem of calculating cavity shapes and drags for arbitrary slender bodies is reduced to one of quadratures. As an example, calculations are made for the family of wedge profiles and results are shown to be in good agreement with "exact" theory results for sufficiently slender bodies. In particular, the example demonstrates that the linearized theory is a valid first order theory.

INTRODUCTION

The problem of practical importance being considered here is that of finding the flow characteristics, and in particular the cavity shape and body drag which result when a two-dimensional body, symmetric with respect to the flow direction, is immersed in a uniform, infinite, steady stream for which it is assumed that cavitation occurs for a certain sufficiently low fluid pressure. The slender body is considered to be of almost arbitrary shape, it only being specified, for the sake of reality, that the body not be of a shape such that the velocity at any forward point on the body exceed that at the cavity separation point. It has been found experimentally that the flow about a cavitating body under the above circumstances involves a trailing cavity of essentially constant interior pressure whose length is dependent upon that pressure and that Froude and Reynolds effects are very often of second order of importance. The pertinent hydrodynamic problem which might be expected to have a physically meaningful solution would be stated thus: To find a (or the) closed (in the finite plane or at infinity) symmetric streamline(s) whose foreshape is given and on whose after part (called the free streamline) the flow velocity or, equivalently, the fluid pressure is a given constant, the flow field exterior to the symmetric closed streamline being time independent, irrotational, incompressible, and single valued. Mathematical investigations of this problem have led to the following important result: Only in the case where the streamline is closed at infinity (called a Helmholtz flow) does a solution to the above problem exist. The existing solution is unique and for it the velocity on the free streamline must equal the velocity of the uniform stream at infinity. Birkhoff¹ has called the nonexistence part of this result Brillouin's Paradox. The fact that the flow conditions at the rear of a finite cavity are not ideal as described in the problem leads to a resolution of the paradox.

¹References are listed on page 20.

In order to obtain, then, some information about finite closed cavities, which are known to occur physically, it has become necessary to investigate not the problem set above, but approximations to that problem involving the so-called finite cavity models. The prominent models are those of Riabouchinsky and Wagner,¹ their justification being that the nonidealness of the flow at the near of the cavity may be approximated quite roughly while reasonable results may still be obtained for the drag of the body and the shape of the forepart of the cavity. The fact that the two different models lead to almost identical results for body drag² lends considerable force to the justification argument.

At the present time, the use of neither cavitation model allows even an approximate solution to be obtained for an arbitrary body; solutions for even those simple bodies treated are obtained at the expense of (relatively speaking) considerable labor. Because of these reasons it seems appropriate that a suitable linearized approximation to the exact problem be discussed. The discussion must thus be limited to the case of slender bodies, but these are bodies of great practical interest.

THE LINEARIZED THEORY

The history of attempts to solve hydrodynamic problems by means of linearizing assumptions is about as old as the history of mathematical hydrodynamics. The linearization of both equations of motion and boundary conditions is, for instance, essential in a great part of the classical theory of waves. Probably the first discussion of a linearized theory of flow past a practical configuration was given by J.H. Michell in 1898 in his now famous analysis of "The Wave-Resistance of a Ship."³ Michell made, as a matter of fact, linearizing assumptions very similar to those which are made in the present paper on cavitation flows. Despite certain similarities between the problems, the present method of solution does not resemble that of Michell who used a Fourier series development. Here the boundary conditions are satisfied by making use of a suitable singularity distribution. The integral equation that results and which must be solved for the determination of the suitable singularity distribution is identical with that which occurs in the linearized theory of lifting airfoils. This theory was apparently first suggested by L. Prandtl about 1918.⁴ Certain results of the thin airfoil theory and in particular the inversion formula of A. Betz (1919)⁵ for the important integral equation will be utilized.

Consider the flow schematically illustrated in Figure 1 and let

$$\vec{V} = \text{Velocity of fluid at any point in the flow field} = U_{\infty} + \vec{v}$$

$$\vec{v} = \text{Perturbation velocity}$$

$$u, v = x \text{ and } y \text{ components, respectively, of } \vec{v}$$

$$U_{\infty} = \text{Uniform velocity at } \infty, \text{ parallel to the } x\text{-axis}$$

$$U_c = \text{Component in } x\text{-direction of velocity on cavity wall} = U_{\infty} + u(x, y_c)$$

p = Local static pressure

p_∞ = Static pressure of stream at infinity

p_c = Cavity pressure

p_o = Pressure on the body

σ = Cavitation number = $\frac{p_\infty - p_c}{\frac{1}{2}\rho U_\infty^2}$

ρ = Constant fluid density

ϕ = Perturbation velocity potential such that $\vec{v} = \nabla \phi$

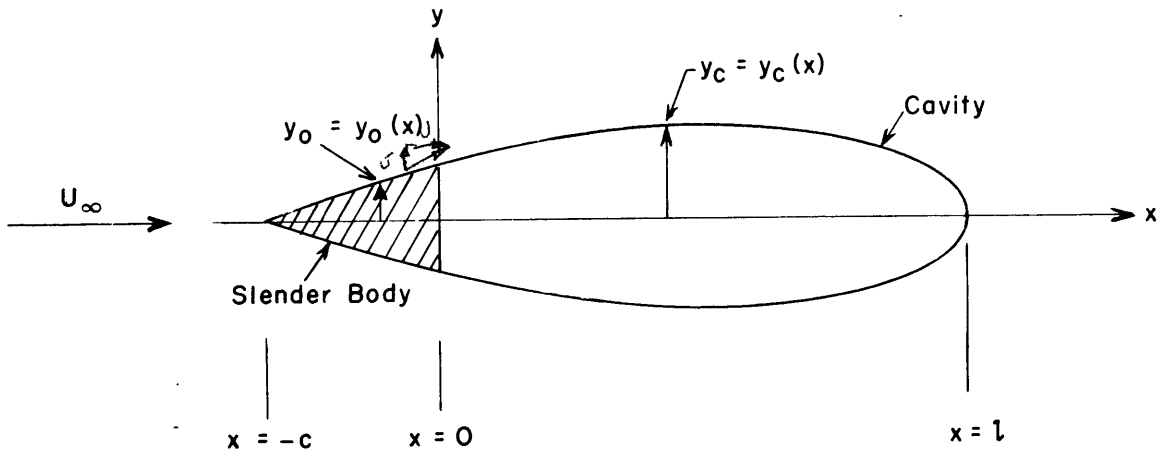


Figure 1 - Schematic Cavitation Flow

On the solid boundary the streamline slope is specified

$$\frac{dy_o}{dx}(x) = \frac{v(x, y_o)}{U_\infty + u(x, y_o)} = \frac{v(x, y_o)}{U_c} \left[1 - \frac{u(x, y_o) - u(x, y_c)}{U_c} + O\left(\frac{v(x, y_o) - u(x, y_c)}{U_c}\right)^2 \right] \quad [1]$$

Where the velocity U_c has been used as a nondimensionalizing factor because theoretical and experimental results indicate that the velocities on the cavitating body are nearly proportional to U_c . This fact has led to the statement of the "principle of stability of the pressure coefficient." (Reference 1, page 66).

On the cavity wall the static pressure is specified as constant = p_c or, equivalently, the cavitation number σ is specified. From Bernoulli's equation it follows that

$$\left\{ \sigma = \frac{2u(x, y_c)}{U_\infty} + O\left(\frac{v(x, y_c)}{U_\infty}\right)^2 = 2\left(\frac{U_c}{U_\infty} - 1\right) + O\left(\frac{v(x, y_c)}{U_\infty}\right)^2 \right. \quad [2]$$

From the Cauchy-Riemann equations it may be inferred that the perturbation velocity changes very slowly in space if streamline slopes and curvatures are small, so that some justification exists for satisfying the linearized boundary conditions on the x -axis instead of on the

slender body. At this point it is not profitable to attempt further to justify the linearization but rather to throw the burden of the justification upon a comparison that will finally be made between exact and linearized theory results for particular cases.

The linearized boundary conditions are

$$\frac{dy_0}{dx}(x) = \frac{v(x,0)}{U_c} \quad -c < x < 0 \quad [1a]$$

$$\sigma = \frac{2u(x,0)}{U_\infty} \quad 0 < x < l \quad [2a]$$

Finally, then, the linearized problem may be stated: To find a harmonic function $\phi(x,y)$, symmetric with respect to the x -axis, whose gradient in the limit vanishes everywhere on a circle of sufficiently large radius about the origin, which satisfies the mixed boundary conditions illustrated schematically in Figure 2, and which satisfies the additional condition that

$$\int_{-c}^l \frac{\partial \phi}{\partial y}(x,0) dx = 0$$

The last condition assures that the body be closed, since

$$\frac{dy_0}{dx}(x,0) = \frac{1}{U_c} \frac{\partial \phi}{\partial y}(x,0)$$

The mathematical meaningfulness of the problem is not known *a priori*, but becomes clear as the solution is constructed.

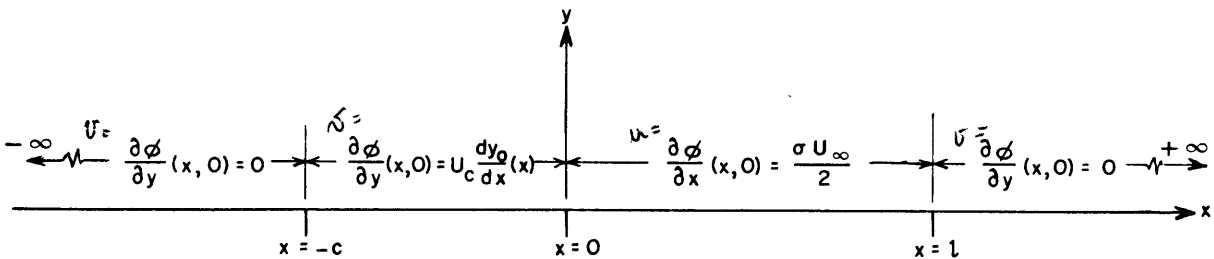


Figure 2 - The Linearized Boundary Conditions

A distribution of sources of strength $m(x)$ along the x -axis for $-c < x < l$ produces a harmonic function with the proper symmetry.

$$\phi(x, y) = \int_{-c}^l \frac{m(x') \ln r \, dx'}{2\pi} \quad \text{where} \quad r = [(x - x')^2 + y^2]^{1/2} \quad [3]$$

$$u(x, y) = \frac{\partial \phi}{\partial x} = \frac{1}{2\pi} \int_{-c}^l \frac{m(x') [x - x'] \, dx'}{[(x - x')^2 + y^2]} \quad [4]$$

$$v(x, y) = \frac{\partial \phi}{\partial y} = \frac{1}{2\pi} \int_{-c}^l \frac{m(x') y}{[(x - x')^2 + y^2]} \, dx' \quad [5]$$

It may easily be shown that

$$u(x, 0) = \frac{1}{2\pi} \int_{-c}^l \frac{m(x') \, dx'}{(x - x')} \quad [6]$$

and, using the substitution $\tan \rho = \frac{x - x'}{y}$,

$$v(x, 0) = \frac{m(x)}{2} \quad [7]$$

For the integral in Equation [6] Cauchy's principal value must be taken. This is true for all improper integrals appearing in the present analysis despite the omission of specific symbolism to that effect.

The mixed boundary conditions on the x -axis will be satisfied if

$$m(x) = 2U_c \frac{dy_0}{dx}(x) \quad -c < x < 0 \quad [8]$$

and

$$\frac{1}{2\pi} \int_{-c}^0 \frac{2U_c \frac{dy_0}{dx'}(x') \, dx'}{(x - x')} + \frac{1}{2\pi} \int_0^l \frac{m(x') \, dx'}{(x - x')} = \frac{U_\infty \sigma}{2} \quad 0 < x < l \quad [9]$$

where Equation [8] has already been incorporated in Equation [9], which is an integral equation for the remaining unknown part of the source distribution. The problem may then be reformulated: To find $m(x)$ such that

$$\int_0^l \frac{m(x') \, dx'}{(x - x')} = \pi \sigma U_\infty - 2U_c \int_{-c}^0 \frac{\frac{dy_0}{dx'}(x') \, dx'}{(x - x')} = f(x) \quad [9a]$$

and

$$\int_0^l m(x') dx' = - \int_{-c}^0 2U_c \frac{dy_0}{dx'}(x') dx' = - 2U_c y(0) \quad [10]$$

THE THIN AIRFOIL THEORY AND THE JUNCTURE CONDITION

Equation [10] requires that the sum of the distributed source strengths be zero or, equivalently, that the body be closed. Equation [9a] has the form of the fundamental integral equation of the thin airfoil theory⁶ where $m(x')$ would there be replaced by (in Glauert's notation) $k(x')$ which is the strength of the distributed vorticity and where $f(x)$ depends upon the shape of the airfoil camber line and the airfoil angle of attack. That problem of the thin airfoil theory which is entirely equivalent to the present problem would be stated: To find a distribution of vorticity in the interval $0 < x < l$ such that the streamline shape in the vicinity of that interval coincides with the shape of the airfoil camber line and such that the lift on the airfoil

$$\left(\rho U_\infty \int_0^l k(x') dx' \right) \parallel$$

is equal to a certain prescribed value.

Now it is a well-known result of both the exact and thin airfoil theories that the airfoil shape and attitude being known, a flow may be found such that the airfoil lift assumes any prescribed value. Thus the thin airfoil problem stated above and, equivalently, the linearized cavitation problem (Equations [9a] and [10]) always have a solution. This result is somewhat paradoxical, since according to our physical experience the lift on an airfoil of particular shape and attitude is quite well determined, and for a given cavitating body there seems to exist a nonarbitrary correspondence between cavity length and cavitation number. In the case of the airfoil the paradoxical result is due entirely to an oversimplification of a physical nature (it is not due to the linearization) and is resolved by invoking the Joukowski condition that the flow leave the trailing edge smoothly, which in the thin airfoil theory takes the form of a further specification that the vorticity strength vanish at the airfoil trailing edge.

In the case of the cavitating body the paradoxical result is due entirely to mathematical oversimplification introduced with the linearizing assumptions. That the linearized form of a cavitation type boundary value problem may have a solution although the solution does not exist for the exact form of the same problem is easily demonstrated by introduction of the following problem: To find a closed body, symmetric with respect to the flow direction, and of such a shape that the pressure is everywhere constant on the body surface. Now it follows from Brillouin's Paradox that such a body does not exist, and yet it is easily shown that a linearized solution exists and that, in fact, elliptic cylinders are the bodies sought. To speak very loosely, the linearized theory produces some approximate solutions which almost, but

not quite, exist in an exact sense. These false solutions must be eliminated from consideration, and this may be done in the case of the cavitation problem by adding the following "junction condition."

The flow at the body-cavity juncture must be "smooth," or, more specifically, the slope of the cavity must be continuous with the slope of the body. In the analysis that follows, this condition will be enforced by eliminating those linearized solutions for the cavity source distribution which "blow-up" at the juncture. The paradoxical result that had at first appeared will thus be resolved, and, as in reality, a nonarbitrary correspondence between cavity length and cavitation number will be obtained.

The admissible linearized flows that remain still exist in contradiction to the Brillouin Paradox, for they are flows about closed bodies with constant pressure afterparts. Their existence is explained by pointing out that the linearized theory is invalid near the end of the cavity where the cavity has roughly an elliptical shaped trailing end, and the real flows corresponding to the linearized flows do not, of course, have constant pressure there.

It is to be emphasized that the use of linearized theory makes unnecessary the selection of a specific finite cavity model.

THE GENERAL SOLUTION FOR THE SOURCE DISTRIBUTION AND CAVITY SHAPE

The solution of the integral Equation [9a] for the cavity source distribution is (see Reference 5, Table of Singular Integral Equations and their Solutions)

$$m(x) = -\frac{1}{\pi^2 \sqrt{x(l-x)}} \left\{ \int_0^l \frac{\sqrt{x'(l-x')}}{(x-x')} \left[\pi \sigma U_\infty - \int_{-c}^0 \frac{2U_c \frac{dy_0}{dt} dt}{(x'-t)} \right] dx' + a \right\} \quad [11]$$

To satisfy the juncture condition it is necessary that the term in brackets in Equation [11] vanish at $x = 0$, i.e.,

$$a + \int_0^l \frac{\sqrt{x'(l-x')}}{-x'} \pi \sigma U_\infty dx' - \int_0^l \frac{\sqrt{x'(l-x')}}{-x'} dx' \int_{-c}^0 \frac{2U_c \frac{dy_0}{dt} dt}{(x'-t)} = 0 \quad [12]$$

so that

$$m(x) = -\frac{\sqrt{x}}{\pi^2 \sqrt{l-x}} \left\{ \int_0^l \frac{\sqrt{l-x'}}{\sqrt{x'}(x-x')} \left[\pi \sigma U_\infty - \int_{-c}^0 \frac{2U_c \frac{dy_0}{dt} dt}{(x'-t)} \right] dx' \right\} \quad [13]$$

or, using Equations [32] and [33] of Appendix 1, Part A

$$m(x) = -\frac{\sigma U_\infty \sqrt{x}}{\sqrt{l-x}} + \frac{\sqrt{x}}{\pi \sqrt{l-x}} \int_{-c}^0 2 U_c \frac{dy_0}{dt} \frac{\sqrt{l-t}}{(x-t)\sqrt{-t}} dt \quad [13a]$$

The cavity shape may now easily be found, since

$$\begin{aligned} y_c(x) &= y_0(0) + \int_0^x \frac{dy_c}{dX} dX = y_0(0) + \frac{1}{2U_c} \int_0^x m(X) dX \\ \therefore y_c(x) - y_0(0) &= -\frac{\sigma U_\infty}{2U_c} \int_0^x \frac{\sqrt{X}}{\sqrt{l-X}} dX + \frac{1}{\pi} \int_{-c}^0 \frac{dy_0}{dt} \frac{\sqrt{l-t}}{\sqrt{-t}} dt \int_0^x \frac{\sqrt{X} dX}{\sqrt{l-X}(X-t)} \\ y_c(x) - y_0(0) &= -\frac{\sigma U_\infty}{2U_c} \left[l \tan^{-1} \sqrt{\frac{x}{l-x}} - \sqrt{x} \sqrt{l-x} \right] \\ &\quad + \frac{2}{\pi} \int_{-c}^0 \frac{dy_0}{dt} \frac{\sqrt{l-t}}{\sqrt{-t}} \left[\sin^{-1} \sqrt{\frac{x}{l}} - \sqrt{\frac{t}{t-l}} \tan^{-1} \sqrt{\frac{x(t-l)}{t(l-x)}} \right] dt \end{aligned} \quad [14]$$

where Equation [30] of Appendix 1, Part A, has been used.

In order that the cavity be closed, Equation [10]:

$$y_c(l) = 0 = -\frac{\sigma U_\infty}{2U_c} \frac{l\pi}{2} + \int_{-c}^0 \frac{dy_0}{dt} \frac{\sqrt{l-t}}{\sqrt{-t}} dt \quad [15]$$

But

$$\frac{U_c}{U_\infty} = 1 + \frac{\sigma}{2}$$

So that (for a given body) the unique relationship between the cavitation number and cavity length is finally obtained:

$$\frac{\sigma}{1 + \frac{\sigma}{2}} = \frac{4}{\pi l} \int_{-c}^0 \frac{dy_0}{dt} \frac{\sqrt{l-t}}{\sqrt{-t}} dt \quad [16]$$

Equation [16] may be used to simplify Equation [14]

$$\begin{aligned} y_c(x) &= \frac{\sigma}{1 + \frac{\sigma}{2}} \left[l \sin^{-1} \sqrt{\frac{x}{l}} + \sqrt{x} \sqrt{l-x} \right. \\ &\quad \left. + l \tan^{-1} \sqrt{\frac{l-x}{x}} - \frac{l\pi}{2} \right] + \frac{2}{\pi} \int_{-c}^0 \frac{dy_0}{dt} \tan^{-1} \sqrt{\frac{t(l-x)}{x(t-l)}} dt \end{aligned} \quad [14a]$$

or

$$y_c(x) = \frac{\sigma l}{2\left(1 + \frac{\sigma}{2}\right)} \left[\sqrt{\frac{x}{l}} \sqrt{1 - \frac{x}{l}} \right] + \frac{2}{\pi} \int_{-c}^0 \frac{dy_0}{dt} \tan^{-1} \sqrt{\frac{t(l-x)}{x(t-l)}} dt \quad [14b]$$

The first term on the right of Equation [14b] represents an elliptical shape of length l and fineness ratio

$$\frac{2\left(1 + \frac{\sigma}{2}\right)}{\sigma}$$

The contribution of the second term is largest just behind the cavitating body, and becomes small at the rear of the cavity. For small cavitation numbers the after shape of the cavity is very nearly of elliptical shape. The cavity then has the shape shown schematically in Figure 3.

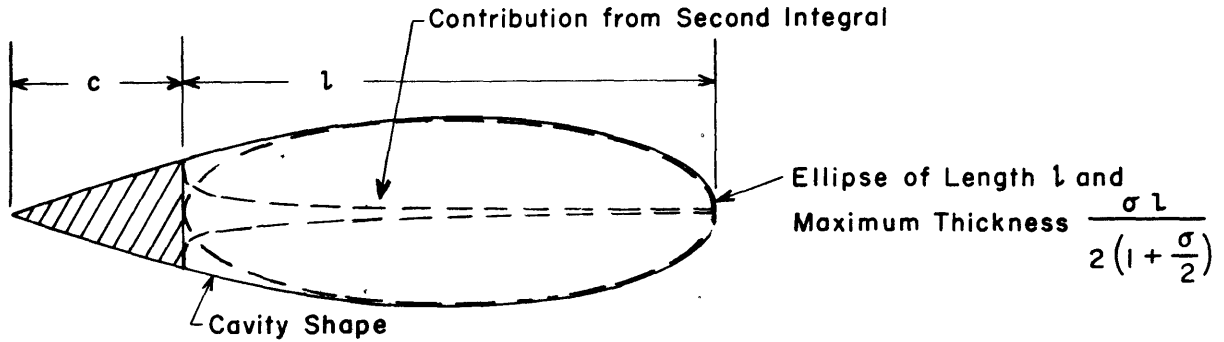


Figure 3 - Cavity Shape for Small Cavitation Numbers

The position of maximum cavity width is obtained at the position where the cavity source strength is zero. From Equation [13a]

$$\frac{\sigma U_\infty \pi}{2U_c} = \int_{-c}^0 \frac{dy_0}{dt} \frac{\sqrt{l-t}}{\sqrt{-t(\bar{x}-t)}} dt$$

where $y(\bar{x})$ is the maximum cavity width. Using Equation [16] it may then be shown that

$$\frac{l}{2} - c < \bar{x} < \frac{l}{2} \quad [14c]$$

and

$$y_c(\bar{x}) \approx \frac{\sigma l}{4\left(1 + \frac{\sigma}{2}\right)} \quad [14d]$$

For small values of σ , it may be shown, using Equation [16], that

$$\sigma \rightarrow 0 \quad \sqrt{l} = \frac{4}{\pi \sigma} \int_{-c}^0 \frac{dy_0}{dt} \frac{dt}{\sqrt{-t}} \quad [16a]$$

THE CALCULATION OF THE CAVITATION DRAG

If the drag of the cavitating body is D , then

$$D = 2 \int_{-c}^0 (p_0 - p_c) \frac{dy_0}{dt} dt = \rho [U_c^2 + v_c^2] \int_{-c}^0 \left[1 - \frac{(U_0^2 + v_0^2)}{U_c^2} \right] \frac{dy_0}{dt} dt \quad [17]$$

Equation [17] may also be written

$$D = \rho [U_c^2 + v_c^2] \int_{-c}^0 \left[-\frac{2}{U_c} (U_0 - U_c) - \left(\frac{U_0 - U_c}{U_c} \right)^2 - \frac{v_0^2}{U_c^2} \right] \frac{dy_0}{dt} dt \quad [17a]$$

After linearization, Equation [17a] becomes

$$D = -2\rho U_c \int_{-c}^0 [u(t, y_0) - u(t, y_c)] \frac{dy_0}{dt} dt \quad [17b]$$

But

$$u(t, y_0) = u_{0-0}(t, y_0) + u_{c-0}(t, y_0),$$

where $u_{0-0}(t, y_0)$ is the x component of that part of the disturbance velocity on the body which is induced by the body source distribution, and $u_{c-0}(t, y_0)$ is the x component of that part of the disturbance velocity on the body which is induced by the cavity source distribution, thus:

$$D = -2\rho U_c \int_{-c}^0 [u_{0-0}(t, y_0) + u_{c-0}(t, y_0) - u(t, y_c)] \frac{dy_0}{dt} dt \quad [17c]$$

It is easily shown that
$$\int_{-c}^0 u_{0-0}(t, y_0) \frac{dy_0}{dt} dt = 0$$

so finally, remembering that
$$u(t, y_c) = \frac{\sigma U_\infty}{2}$$

$$D = 2\rho U_c \left\{ \frac{\sigma U_\infty}{2} y_0(0) - \int_{-c}^0 u_{c-0}(t, y_0) \frac{dy_0}{dt} dt \right\} \quad [17d]$$

The integral on the right hand side of Equation [17d] is easily determined from Equations [6] and [11], using Equations [31] and [34] of Appendix 1, Part A:

$$\int_{-c}^0 2U_c \frac{dy_0}{dt} u_{c-0}(t) dt = \sigma U_c U_\infty y_0(0) - \sigma U_c U_\infty \int_{-c}^0 \frac{dy_0}{dt} \frac{\sqrt{t}}{\sqrt{t-l}} dt$$

$$+ \frac{2U_c^2}{\pi} \int_{-c}^0 \frac{dy_0}{dt} dt \int_{-c}^0 \frac{dy_0}{d\tau} \sqrt{\frac{t(\tau-l)}{\tau(t-l)}} \frac{d\tau}{(t-\tau)}$$
[18]

So, finally, using the result of Appendix 1, Part B:

$$\frac{D}{\frac{1}{2} \rho U_\infty^2} = 2\sigma \sqrt{1+\sigma} \int_{-c}^0 \frac{dy_0}{d\tau} \frac{\sqrt{t}}{\sqrt{t-l}} dt + \frac{2l}{\pi} (1+\sigma) \left[\int_{-c}^0 \frac{dy_0}{dt} \frac{dt}{\sqrt{t(t-l)}} \right]^2$$
[19]

For small σ , it may be shown, using Equation [23b], that

$$\frac{D}{\frac{1}{2} \rho U_\infty^2} \approx \frac{D_{\sigma=0}}{\frac{1}{2} \rho U_\infty^2} (1+\sigma)$$
[19a]

This result is in close agreement with exact calculations for two-dimensional flows based on the re-entrant jet (Wagner) model,^{2,7} and, incidentally, with body of revolution drag measurements.^{8,9}

THE INFINITE CAVITY CASE ($\sigma = 0$)

The case when the cavity is infinite and the cavitation number zero (necessarily) is of particular interest since it has been the subject of many theoretical investigations. It is of interest to see whether certain results of exact theory are also obtained in the present investigation.

The source distribution for the infinite cavity is given by:

$$m(x) = \frac{2U_c \sqrt{x}}{\pi} \int_{-c}^0 \frac{\frac{dy_0}{dt}}{\sqrt{-t}(x-t)} dt$$
[20]

This result was obtained by a solution of the appropriate boundary value problem for $\sigma = 0$ and is identical with the result obtained by taking the limit as $\sigma \rightarrow 0$ in Equation [13a].

The shape of the infinite cavity is easily found from the source distribution, Equation [20], in the same way as the finite cavity shape was found from Equation [13a]:

$$y_c(x) - y_0(0) = \frac{2\sqrt{x}}{\pi} \int_{-c}^0 \frac{dy_0}{dt} \frac{dt}{\sqrt{-t}} - \frac{2}{\pi} \int_{-c}^0 \frac{dy_0}{dt} \tan^{-1} \sqrt{\frac{x}{t}} dt$$
[21]

The asymptotic cavity shape is given by

$$\lim_{x \rightarrow \infty} \frac{y_c(x)}{\sqrt{x}} = \frac{2}{\pi} \int_{-c}^0 \frac{dy_0}{dt} \frac{dt}{\sqrt{-t}} \quad [22]$$

It is to be noted that it has been shown (Reference 1, page 51) that the two-dimensional cavity must have this asymptotic form, i.e.,

$$\lim_{x \rightarrow \infty} \frac{y_c(x)}{\sqrt{x}} = \text{A constant which is a function of the body shape}$$

The cavitation drag may be found in the same way as it was found for the finite cavity case. The result is identical with that obtained by taking the limit of Equation [19] as $\sigma \rightarrow 0$.

$$\frac{D_{\sigma=0}}{\frac{1}{2} \rho U_{\infty}^2} = \frac{2}{\pi} \left[\int_{-c}^0 \frac{dy_0}{dt} \frac{dt}{\sqrt{-t}} \right]^2 \quad [23]$$

But, by using Equation [22], the drag may be written in terms of the asymptotic cavity shape

$$\frac{D}{\frac{1}{2} \rho U^2} = \frac{\pi}{2} \left[\lim_{x \rightarrow \infty} \frac{y_c(x)}{\sqrt{x}} \right]^2 \quad [23a]$$

This is precisely the formula given by Levi-Civita (Reference 1, page 51) for the drag of a symmetric body with infinite cavity. That this result has been obtained is an important justification for the linearized theory.

THE SLENDER WEDGE. COMPARISON WITH EXACT THEORY

In order to evaluate further the meaningfulness of the linearized theory for cavitating flows it is of interest to use it to examine some characteristics of flow about a configuration which has also been treated using more exact theory. Such a flow is that about the wedge profile which has been discussed in detail for zero cavitation number,¹⁰ and which, for nonzero cavitation number, has been discussed through the use of the Riabouchinsky¹¹ and the Wagner² models.

Consider a wedge of chord length c , maximum thickness T , and a half angle γ , as shown in Figure 4.

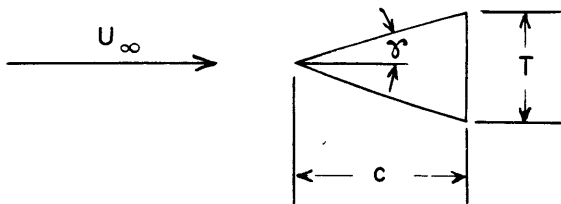


Figure 4 - Wedge Profile

The application of Equations [21], [22], [23c] and [16], respectively, to the wedge flow yields the following linearized theory results:

$$\sigma = 0: \quad y_c = \frac{T}{2} + \frac{2\gamma}{\pi} \left[(x+c) \tan^{-1} \sqrt{\frac{c}{x}} + \sqrt{xc} - \frac{c\pi}{2} \right] \quad [24]$$

$$\sigma = 0: \quad \lim_{x \rightarrow \infty} \frac{y_c(x)}{\sqrt{x}} = \frac{4\gamma\sqrt{c}}{\pi} \quad [25]$$

$$\sigma = 0: \quad C_D = \frac{D}{\frac{1}{2} \rho U_\infty^2 \frac{T}{2}} = \frac{8\gamma}{\pi} \quad [26]$$

$$\sigma > 0: \quad \frac{\sigma}{1 + \frac{\sigma}{2}} = \frac{4\gamma}{\pi} \left\{ \sqrt{\frac{c}{l}} \sqrt{1 + \frac{c}{l}} + \log \left[\sqrt{\frac{c}{l}} + \sqrt{1 + \frac{c}{l}} \right] \right\} \quad [27]$$

The application of exact theory results¹⁰ for $\sigma = 0$ yields:

$$\sigma = 0: \quad \left\{ \begin{array}{l} y_c(\text{exact}) = y_c(\text{linearized}) + O(\gamma^2) \\ \lim_{x \rightarrow \infty} \frac{y_c(x)}{\sqrt{x}} (\text{exact}) = \lim_{x \rightarrow \infty} \frac{y_c(x)}{\sqrt{x}} (\text{linearized}) + O(\gamma^2) \\ C_D(\text{exact}) = C_D(\text{linearized}) + O(\gamma^2) \end{array} \right. [28]$$

The exact result for the drag coefficient is plotted in Figure 5 together with the linearized result, Equation [26]. The linearized theory result for the finite cavity length, Equation [27], is shown in Figure 6 together with the result, as calculated by Plesset and Shaffer¹¹ using the Riabouchinsky model. The finite cavity's maximum diameter as approximated by Equation [14d] is plotted in Figure 7 together with the results of the Plesset and Shaffer calculations.

SUMMARY AND CONCLUSIONS

1. The linearized theory is a meaningful first order theory for calculating flow characteristics about slender two-dimensional forms for positive cavitation numbers. The justification of this conclusion lies in the following results: (a) In the case of wedges at zero cavitation number the linearized result for cavity shape and drag actually is the first order term in an expansion in powers of the wedge angle, (b) for arbitrary bodies at zero cavitation number the same asymptotic cavity shape is obtained according to both the linearized and exact theories,

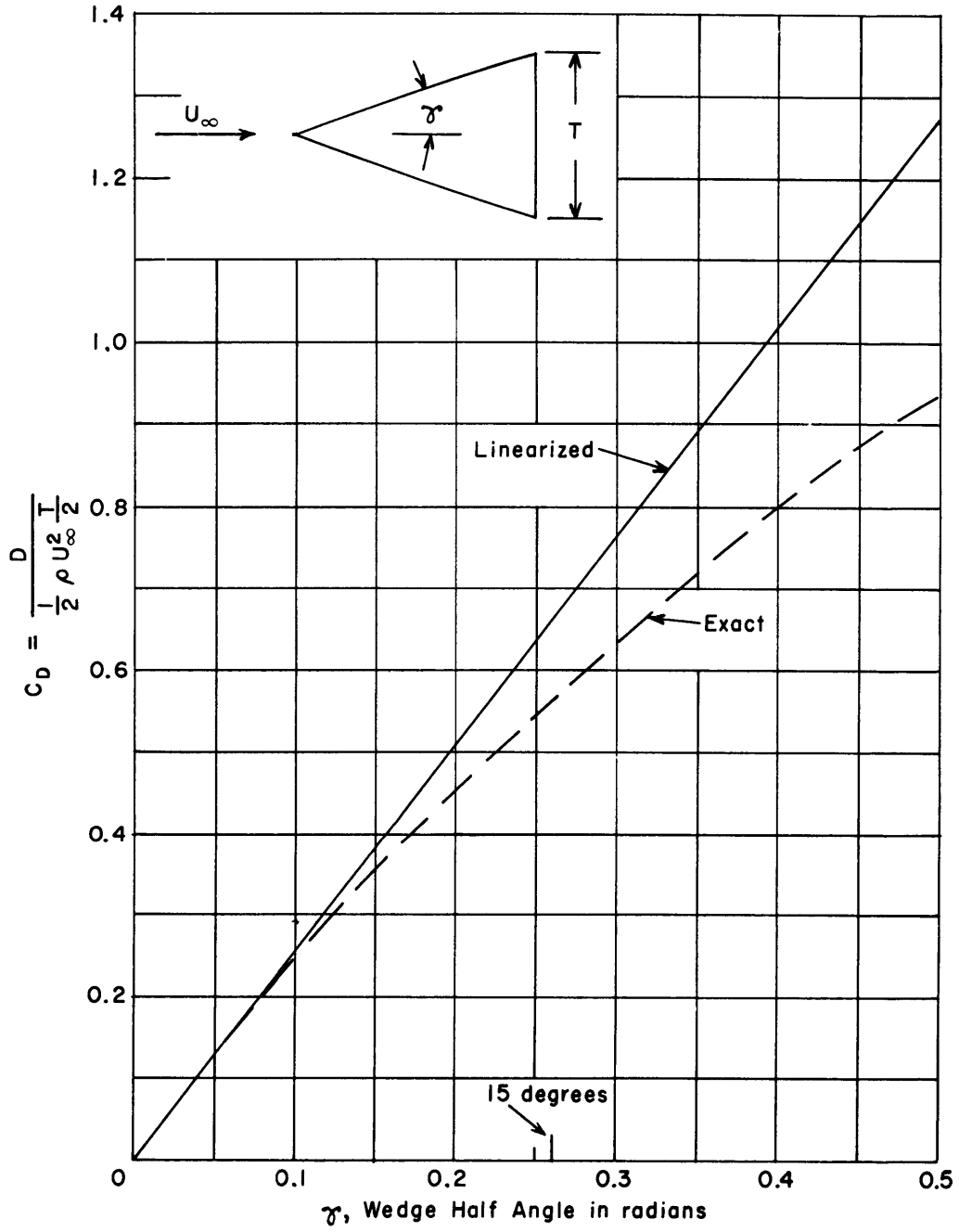


Figure 5 - Cavitation Drag Coefficient for Wedges, $\sigma = 0$

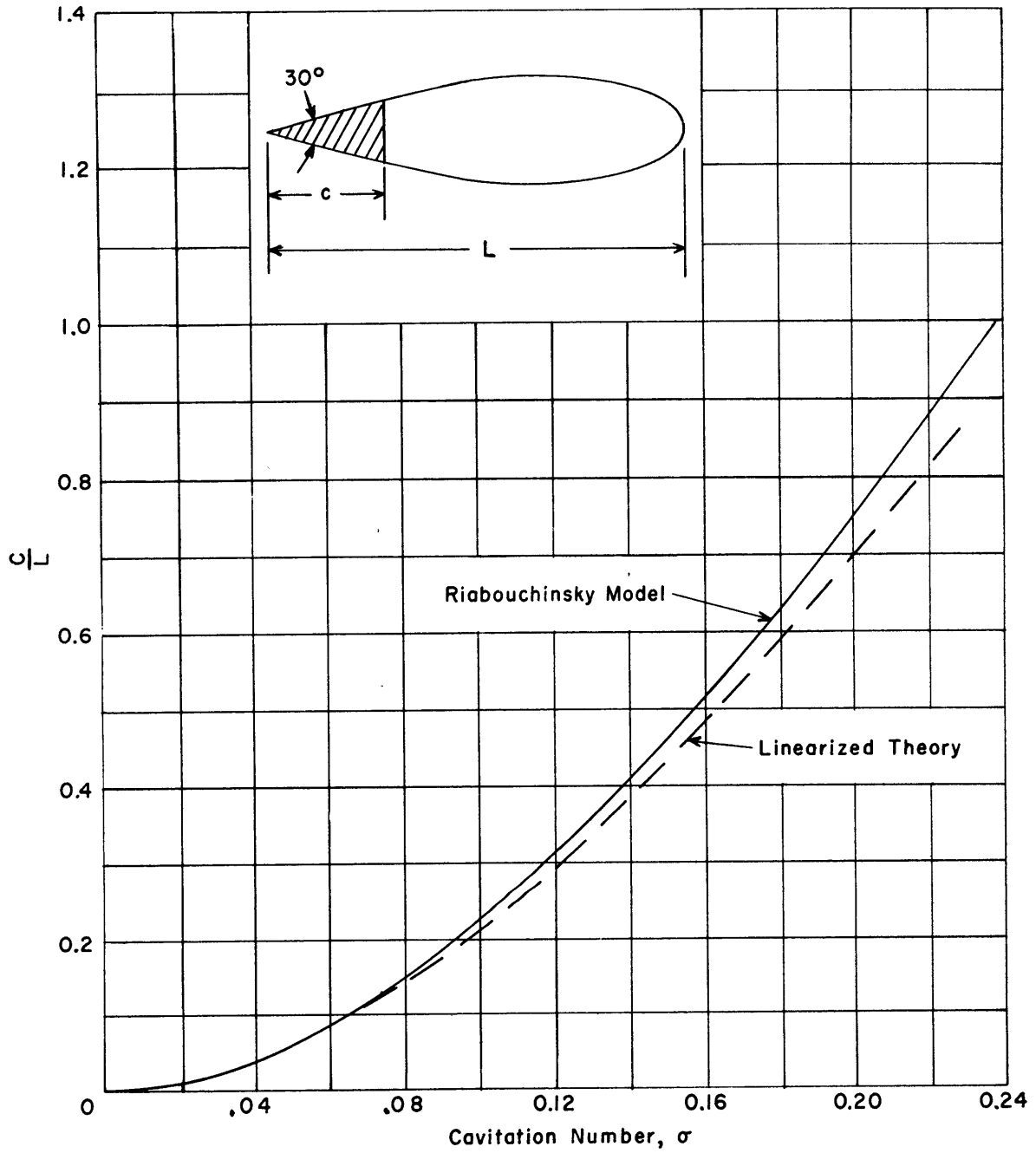


Figure 6 - Cavity Length as a Function of Cavitation Number for a 30-Degree Wedge

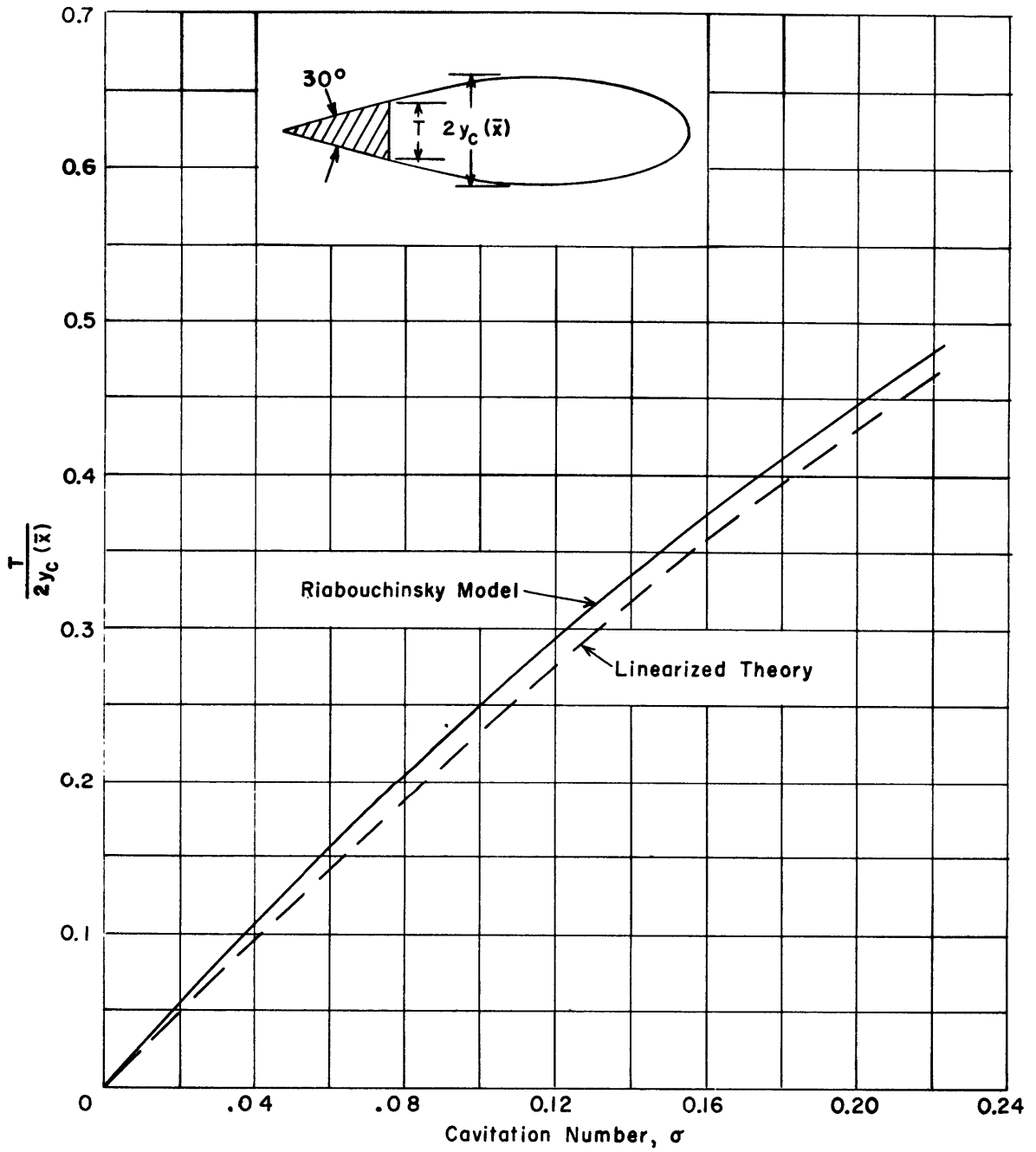


Figure 7 - Maximum Cavity Diameter as a Function of Cavitation Number for a 30-Degree Wedge

and the identical relationship between asymptotic cavity shape and body drag is obtained, and (c) for finite cavities behind wedges the shape of the cavities according to the linearized and Riabouchinsky model theories are in good agreement.

2. The use of the linearized theory obviates the necessity for choosing a finite cavity model. The linearizing assumptions, themselves, permit a meaningful closed cavity solution to be found.

3. The use of the linearized theory reduces the problem of calculating cavity shapes and drags for arbitrary slender bodies (and positive cavitation numbers) to one of quadratures.

4. The shape of finite cavities behind slender bodies is, according to the linearized theory always essentially elliptic, the slenderness of the ellipse being a function of the cavitation number.

APPENDIX I

A. USEFUL INTEGRALS

Certain useful results which can be obtained in a straightforward manner are stated below:

Let

$$I(x', s, X) = \int_0^X \frac{\sqrt{x} dx}{\sqrt{s-x} (x-x')}$$

and let R denote "the real part of". Then

$$I(x', s, X) = 2 \sin^{-1} \sqrt{\frac{X}{s}} \quad [29]$$

$$+ R \left[\sqrt{\frac{x'}{s-x'}} \log \left\{ \frac{(\sqrt{X}-\sqrt{x'}) (\sqrt{s-X} \sqrt{s-x'} + s + \sqrt{X} \sqrt{x'})}{(\sqrt{X}+\sqrt{x'}) (\sqrt{s-X} \sqrt{s-x'} + s - \sqrt{X} \sqrt{x'})} \right\} \right]$$

$$(for \ x' < 0) \ I(x', s, X) = 2 \sin^{-1} \sqrt{\frac{X}{s}} \quad [30]$$

$$- \sqrt{\frac{x'}{x'-s}} \left(\pi + 2 \tan^{-1} \frac{\sqrt{X|x'|}}{s + \sqrt{s-X} \sqrt{s+|x'|}} - 2 \tan^{-1} \sqrt{\frac{|x'|}{X}} \right)$$

$$I(x', s, s) = \pi + R \left[\sqrt{\frac{x'}{s-x'}} (i\pi) \right] = \begin{cases} \pi & for \ s > x' > 0 \\ \pi \left(1 - \sqrt{\frac{x'}{x'-s}} \right) & for \ x' > s \\ & or \ x' < 0 \end{cases} \quad [31]$$

$$\int_0^s \frac{\sqrt{s-x}}{\sqrt{x} (x'-x)} dx = I(s-x', s, s) = \pi \ (for \ s > x' < 0) \quad [32]$$

$$\int_0^s \frac{\sqrt{s-x} dx}{\sqrt{x} (x'-x) (x-t)} = \frac{1}{(x'-t)} \left[I(s-x', s, s) - I(s-t, s, s) \right] \quad [33]$$

$$= (for \ 0 < x' < s) \frac{\pi}{(x'-t)} \sqrt{\frac{t-s}{t}}$$

$$\int_0^s \frac{\sqrt{x} dx}{\sqrt{s-x} (t-x) (x-\tau)} = \frac{1}{(t-\tau)} \left[I(\tau, s, s) - I(t, s, s) \right] \quad [34]$$

$$= (for \ \tau < 0) \frac{\pi}{(t-\tau)} \left[\sqrt{\frac{t}{t-s}} - \sqrt{\frac{\tau}{\tau-s}} \right]$$

B. A PROOF OF A RESULT USED IN THE DERIVATION OF EQUATION [19]

It is to be proved that

$$J = \int_{-c}^0 \int_{-c}^0 \frac{dy_0}{dt} \frac{dy_0}{d\tau} \sqrt{\frac{\tau-l}{t-l} \cdot \frac{t}{\tau}} \frac{dt d\tau}{t-\tau} = -\frac{l}{2} \left[\int_{-c}^0 \frac{dy_0}{dt} \frac{dt}{\sqrt{t(t-l)}} \right]^2$$

but

$$\begin{aligned} J &= \int_{-c}^0 \int_{-c}^0 \frac{dy_0}{d\tau} \frac{dy_0}{dt} \sqrt{\frac{t-l}{\tau-l} \cdot \frac{\tau}{t}} \frac{d\tau dt}{\tau-t} \\ &= \frac{1}{2} \int_{-c}^0 \int_{-c}^0 \frac{dy_0}{dt} \frac{dy_0}{d\tau} \left[\sqrt{\frac{\tau-l}{t-l} \cdot \frac{t}{\tau}} - \sqrt{\frac{t-l}{\tau-l} \cdot \frac{\tau}{t}} \right] \frac{dt d\tau}{t-\tau} \\ &= -\frac{l}{2} \int_{-c}^0 \int_{-c}^0 \frac{dy_0}{dt} \frac{dy_0}{d\tau} \frac{dt d\tau}{\sqrt{t\tau(l-t)(l-\tau)}} \\ &= -\frac{l}{2} \left[\int_{-c}^0 \frac{dy_0}{dt} \frac{dt}{\sqrt{t(t-l)}} \right]^2 \end{aligned}$$

C. LISTING OF USEFUL THEORETICAL RESULTS

The most useful theoretical results are, for convenience, listed below:

Relationship between Cavitation Number and Cavity Length:

$$\frac{\sigma}{1 + \frac{\sigma}{2}} = \frac{4}{\pi l} \int_{-c}^0 \frac{dy_0}{dt} \frac{\sqrt{l-t}}{\sqrt{-t}} dt \quad [16]$$

The Cavity Shape:

$$y_c(x) = \frac{\sigma l}{2 \left(1 + \frac{\sigma}{2}\right)} \left[\sqrt{\frac{x}{l}} \sqrt{1 - \frac{x}{l}} \right] + \frac{2}{\pi} \int_{-c}^0 \frac{dy_0}{dt} \tan^{-1} \sqrt{\frac{t(l-x)}{x(t-l)}} dt \quad [14b]$$

The Cavity Shape for $\sigma = 0$:

$$y_c(x) - y_0(0) = \frac{2\sqrt{x}}{\pi} \int_{-c}^0 \frac{dy_0}{dt} \frac{dt}{\sqrt{-t}} - \frac{2}{\pi} \int_{-c}^0 \frac{dy_0}{dt} \tan^{-1} \sqrt{\frac{-x}{t}} dt \quad [21]$$

Approximate Solution for the Maximum Cavity Semi-Thickness:

$$y_c(\bar{x}) = \frac{\sigma l}{4 \left(1 + \frac{\sigma}{2}\right)} \quad [14d]$$

Cavitation Drag:

$$\frac{D}{\frac{1}{2} \rho U_{\infty}^2} = 2\sigma \sqrt{1+\sigma} \int_{-c}^0 \frac{dy_0}{dt} \frac{\sqrt{t}}{\sqrt{t-l}} dt + \frac{2l}{\pi} (1+\sigma) \left[\int_{-c}^0 \frac{dy_0}{dt} \frac{dt}{\sqrt{t(t-l)}} \right]^2 \quad [19]$$

Approximate Solution for Cavitation Drag for Small σ :

$$D \approx D_{\sigma=0} (1+\sigma) \quad [19a]$$

Cavitation Drag for $\sigma = 0$:

$$\frac{D}{\frac{1}{2} \rho U_{\infty}^2} = \frac{2}{\pi} \left[\int_{-c}^0 \frac{dy_0}{dt} \frac{dt}{\sqrt{-t}} \right]^2 \quad [23b]$$

REFERENCES

1. Birkhoff, G., "Hydrodynamics," Princeton University Press for University of Cincinnati, 1950.
2. Gilbarg, D. and Rock, D.H., "On Two Theories of Plane Potential Flows with Finite Cavities," Naval Ordnance Laboratory Memorandum 8718, 29 August 1946.
3. Michell, J.H., "The Wave-Resistance of a Ship," Philosophical Magazine (45), 1898.
4. Birnbaum, "Die tragende Wirbelfläche als Hilfsmittel zur Behandlung des ebenen Problems der Tragflügeltheorie," ZAMM, 1923.
5. Schmeidler, Werner, "Integralgleichungen mit Anwendungen in Physik und Technik, Vol. I," Akademische Verlagsgesellschaft, Gust und Fortig, E.-G., Leipzig, Germany, 1950.
6. Glauert, H., "The Elements of Aerofoil and Airscrew Theory," The Macmillan Company, New York, N.Y., 1944.
7. Arnoff, E.L., "Re-entrant Jet Theory and Cavity Drag for Symmetric Wedges," U.S. Naval Ordnance Test Station Report 368, NavOrd Report 1298, China Lake, California, 21 March 1951.
8. Reichardt, H., "The Laws of Cavitation Bubbles at Axially Symmetric Bodies in a Flow," Reports and Translations Number 766, Ministry of Aircraft Production, 15 Aug., 1946 (Distributed in U.S. by the Office of Naval Research, Wash., D.C.).
9. Eisenberg, P., "On the Mechanism and Prevention of Cavitation," TMB Report 712, July 1950 (An Addendum to TMB Report 712 has been published as TMB Report 842, October 1952).

10. Milne-Thomson, L.M., "Theoretical Hydrodynamics," Second Edition, The Macmillan Company, New York, N.Y., 1950.

11. Plesset, M.S. and Shaffer, P.A., "Cavity Drag in Two and Three Dimensions," U.S. Naval Ordnance Test Station Report 131, NavOrd Report 1014. Inyokern, Calif., 6 October 1949.

INITIAL DISTRIBUTION

Copies

- 12 Chief, Bureau of Ships, Technical Library (Code 327), for distribution:
 - 5 - Technical Library (Code 327)
 - 2 - Applied Science (Code 370)
 - 2 - Propellers and Shafting (Code 554)
 - 1 - Preliminary Design (Code 420)
 - 1 - Ship Design (Code 410)
 - 1 - Machinery Design (Code 430)
- 4 Chief, Bureau of Ordnance, Underwater Ordnance (Re6a)
- 3 Chief, Bureau of Aeronautics, Aero and Hydrodynamics (DE-3)
- 4 Chief of Naval Research
 - 3 - Fluid Mechanics
 - 1 - Undersea Warfare
- 4 Commander, Naval Ordnance Laboratory, White Oak, Silver Spring 19, Md.
- 3 Commander, Naval Ordnance Test Station, Underwater Ordnance Division, Pasadena Annex, Pasadena, Calif.
- 1 Commanding Officer, Navy Underwater Sound Laboratory, New London, Conn.
- 1 Commanding Officer and Director, U.S. Navy Electronics Laboratory, San Diego 52, Calif.
- 1 Commanding Officer, U.S. Naval Underwater Ordnance Station, Newport, R.I.
- 1 Commander, Philadelphia Naval Shipyard (Code 263), Naval Base, Phila. 12, Pa.
- 1 Commander, Portsmouth Naval Shipyard (Code 263 A), Portsmouth, N.H.
- 1 Commanding Officer, Transportation Research and Development Station, Fort Eustis, Va.
- 1 Director, U.S. Coast and Geodetic Survey, Wash. 25, D.C.
- 1 Chief, Division of Preliminary Design, U.S. Maritime Administration, Washington 25, D.C.
- 2 Director, Technical Information Branch, Aberdeen Proving Grounds, Aberdeen, Md.
- 6 Director, National Advisory Committee for Aeronautics, 1724 F St., N.W., Wash., D.C.
- 2 Director, U.S. Waterways Experiment Station, Vicksburg, Miss.
- 1 Director, Woods Hole Oceanographic Institution, Woods Hole, Mass.
- 1 Bureau of Reclamation, Denver Federal Center, Denver, Colo.
- 2 Newport News Shipbuilding and Dry Dock Co., Newport News, Va., for distribution:
 - 1 Mr. J.P. Comstock, Asst. Naval Architect
 - 1 Mr. C.H. Hancock, Hydraulic Laboratory
- 1 New York Shipbuilding Corp., Camden 1, N.J., Attn: Mr. J.W. Thompson, Naval Architect (Design)
- 2 Gibbs and Cox, Inc., 21 West St., New York 6, N.Y., 1 copy for Mr. John P. Breslin
- 1 Sparkman and Stephens, Inc., 11 E. 44th St., New York, N.Y.

Copies

- 2 Director, Ordnance Research Laboratory, Pennsylvania State College, State College, Pa.
- 2 Director, Experimental Towing Tank, Stevens Institute of Technology, 711 Hudson Street, Hoboken, N.J.
- 1 Director, Iowa Institute of Hydraulic Research, State University of Iowa, Iowa City, Iowa
- 1 Director, Hydrodynamic Laboratory, California Institute of Technology, Pasadena 4, Calif.
- 1 Director, St. Anthony Falls Hydraulic Laboratory, University of Minnesota, Minneapolis 14, Minn.
- 1 Dr. Harold Wayland, California Institute of Technology, Pasadena 4, Calif.
- 1 Prof. A. Hollander, California Institute of Technology, Pasadena 4, Calif.
- 2 Dr. A.T. Ippen, Director, Hydrodynamics Laboratory, Department of Civil and Sanitary Engineering, Massachusetts Institute of Technology, Cambridge 39, Mass.
- 1 Head, Department of Naval Architecture and Marine Engineering, Massachusetts Institute of Technology, Cambridge 39, Mass.
- 2 Director, Experimental Naval Tank, Department of Naval Architecture and Marine Engineering, University of Michigan, Ann Arbor, Mich.
- 1 Dr. David Gilbarg, Department of Mathematics, Indiana University, Bloomington, Ind.
- 1 Dr. V.L. Streeter, Illinois Institute of Technology, 3300 Federal Street, Chicago 16, Ill.
- 1 Director, Applied Physics Laboratory, Johns Hopkins University, Silver Spring, Md.
- 1 Prof. W.S. Hamilton, Technological Institute, Northwestern University, Evanston, Ill.
- 1 Prof. Garrett Birkhoff, Harvard University, Cambridge, Mass.
- 1 Prof. K.E. Schoenherr, Dean, School of Engineering, Notre Dame University, Notre Dame, Ind.
- 1 Dr. M.S. Plesset, California Institute of Technology, Pasadena 4, Calif.
- 1 Mr. Walter Daskin, Instructor, Mechanical Engineering Department, Johns Hopkins University, Baltimore, Md.
- 1 Prof. M.B. McPherson, Hydraulics Laboratory, Lehigh University, Bethlehem, Pa.
- 1 Director, Fritz Engineering Laboratory, Lehigh University, Bethlehem, Pa.
- 1 Carnegie Institute of Technology, Schenley Park, Pittsburgh 13, Pa.,
Attn: Library
- 1 Prof. N.M. Newmark, College of Engineering, University of Illinois, Urbana, Ill.
- 1 Prof. Walter L. Moore, Department of Civil Engineering, University of Texas, Austin 12, Texas
- 1 Prof. Carl E. Kindswater, School of Civil Engineering, Georgia Institute of Technology, Atlanta, Ga.
- 1 Prof. Lydik S. Jacobsen, Department of Mechanical Engineering, Stanford University, Calif.

Copies

- 1 Chairman, Graduate Division of Applied Mathematics, Brown University, Providence, R.I.
- 1 Prof. Charles A. Shreeve, Department of Mechanical Engineering, University of Maryland, College Park, Md.
- 1 Prof. A. Weinstein, Instructor of Fluid Dynamics and Applied Mathematics, University of Maryland, College Park, Md.
- 1 Dr. J. Younger, Head, Mechanical Engineering Department, University of Maryland, College Park, Md.
- 1 Prof. J. Vennard, Department of Civil Engineering, Stanford University, Palo Alto, Calif.
- 1 Librarian, American Society of Mechanical Engineers, 29 West 39th Street, New York 18, N.Y.
- 1 Librarian, American Society of Civil Engineers, 33 West 39th Street, New York 18, N.Y.
- 1 Librarian, Franklin Institute of the State of Pennsylvania, Philadelphia 3, Pa.
- 1 Reed Research, Inc., 1048 Potomac Street, N.W., Washington 7, D.C.
- 1 Librarian, Carbide and Carbon Chemicals Co., UCC, K-25 Plant, P.O. Box P, Oak Ridge, Tenn.
- 1 Librarian, Rensselaer Polytechnic Institute, Troy, N.Y.
- 1 Vickers, Inc., Division of Sperry Corp., 14544 Third Ave., Highland Park 3, Mich.
- 1 Cornell Aeronautical Laboratory, Inc., 4455 Genesee Street, Buffalo 21, N.Y.
- 1 James Forrestal Research Center, Princeton University, Princeton, N.J.,
Attn: Mr. Maurice H. Smith, Research Associate
- 1 Pacific Aeronautical Library, 7660 Beverly Blvd., Los Angeles 36, Calif.
- 1 Consolidated Vultee Aircraft Corp., San Diego 12, Calif., Attn: Engineering Library
- 1 Friede and Goldman, Inc., Naval Architects and Marine Engineers, 1420 National Bank of Commerce Building, New Orleans 12, La.
- 1 Mr. Kent C. Thorton, Naval Architect, American Shipbuilding Co., Foot of W. 54th Street, Cleveland 2, Ohio
- 1 Editor, Aeronautical Engineering Review, 2 E. 64th St., New York 21, N.Y.
- 1 Editor, Applied Mechanics Review, Midwest Research Institute, 4049 Pennsylvania, Kansas City 2, Mo.
- 1 Editor, Engineering Index, 29 W. 39th St., New York 18, N.Y.
- 1 Editor, Mathematical Reviews, Brown University, Providence, R.I.
- 9 British Joint Services Mission (Navy Staff), P.O. Box 165, Benjamin Franklin Station, Washington, D.C.
- 8 U.S. Naval Attache and Naval Attache for Air, London, England
- 1 British Shipbuilding Research Association, 5 Chesterfield Gardens, Curzon St., London, W. 1, England

Copies

- 1 Capt. R. Brard, Directeur, Bassin d'Essais des Carènes, 6 Boulevard Victor, Paris (15e) France
- 1 Dr. L. Malavard, Office National d'Etudes et de Recherches Aéronautiques, 25 Avenue de la Division - Le Clerc, Chatillon, Paris, France
- 1 Gen. Ing. U. Pugliese, Presidente, Istituto Nazionale per Studi ed Esperienze di Architettura Navale, via della Vasca Navale 89, Rome, Italy
- 1 Sr. M. Acevedo y Campoamor, Director, Canal de Experiencias Hidrodinámicas, El Pardo, Madrid, Spain
- 1 Dr. J. Dieudonné, Directeur, Institut de Recherches de la Construction Navale, 1 Boulevard Haussmann, Paris (9e), France
- 1 Prof. L. Troost, Superintendent, Nederlandsh Scheepsbouwkundig Proefstation, Haagsteeg 2, Wageningen, The Netherlands
- 1 Prof. J.K. Lunde, Skipsmodelltanken, Tyholt Trondheim, Norway
- 1 Prof. H. Nordstrom, Director, Statens Skeppsprovninganstalt, Göteborg 24, Sweden
- 1 Dr. J.F. Allan, Superintendent, Ship Division, National Physical Laboratory, Teddington, Middlesex, England
- 1 Dr. G. Weinblum, Edmund Siemens Allee 1, Universitaet, Hamburg, Germany
- 1 Prof. N.M. Newmark, College of Engineering, University of Illinois, Urbana, Ill.
- 1 Prof. Walter L. Moore, Department of Civil Engineering, University of Texas, Austin 12, Texas

MIT LIBRARIES DUPL

3 9080 02754 1504

MAY 7 1976

SEP 08 1981

NOV 15 1983

JUL 22 1988